

## Machine Learning-based Tools to Model and to Remove the Off-Target-Effect

Riwal LEFORT · Ludovico FUSCO ·  
Olivier PERTZ · François FLEURET

Accepted: March 2015

**Abstract** A RNA interference, also called a gene knockdown, is a biological technique which consists of inhibiting a targeted gene in a cell. By doing so, one can identify statistical dependencies between a gene and a cell phenotype. However, during such a gene inhibition process, additional genes may also be modified. This is called the “off-target-effect”. The consequence is that there are some additional phenotype perturbations which are “off-target”.

In this paper, we study new machine-learning tools that both model the cell phenotypes and remove the “off-target-effect”.

We propose two new automatic methods to remove the off-target components from a data sample. The first method is based on Vector Quantization (VQ). The second method we propose relies on a classification forest. Both methods rely on analyzing the homogeneity of several repetitions of a gene knockdown. The baseline we consider is a Gaussian Mixture Model (GMM) whose parameters are learned under constraints with a standard Expectation-Maximization algorithm.

We evaluate these methods on a real data set, a semi-synthetic data set, and a synthetic toy data set. The real data set and the semi-synthetic data set are composed of cell growth dynamic quantities measured in time laps movies. The main result is that we obtain the best recognition performance with the probabilistic version of the Vector Quantization-based method.

**Keywords** Vector Quantization · Random forest · Gaussian-Mixture Model · Bioinformatics · Off-target-effect

---

This work was supported by the Swiss National Science Foundation under Sinergia grant 127456 “Understanding Brain morphogenesis”, and from a Human Frontier Science Program grant.

---

R. LEFORT and F. FLEURET  
Idiap Research Institute  
E-mail: riwal.lefort@unicaen.fr

L. FUSCO and O. PERTZ  
University of Basel

## 1 Introduction

### 1.1 The off-target-effect

The analysis of gene functions is a major challenge classically carried out using RNA interference: one can infer the role of a gene by using a RNA molecule that knockdowns its expression, and examine the resulting phenotypical perturbation. For instance, if a cell is smaller after a gene inhibition, one can conclude that the considered gene has an important role regarding the said size. This technique is used for understanding phenomena such as endocytosis [6] and cell migration [2].

However, the gene inhibition technique with RNA remains often imprecise, and may cause the inhibition of additional and non-targeted genes. This phenomenon, which is called the “off-target-effect” [12], may induce some additional changes in the phenotype. For instance, a cell may be smaller after the gene inhibition, but it may also have a greater mobility during its growth, due to a hidden gene inhibition.

In this article, we propose novel machine-learning-based tools to automatically remove the “off-target” components from a data-set of phenotypic measurements.

### 1.2 State-of-the-art

The usual protocol used to study the relation between gene expression and phenotype is as follows [8], [6]: The phenotype obtained with a given RNA molecule is first modeled by a vector each component of which is associated to a particular feature of the cell (related to its morphological, dynamic, or contextual properties) and depends on the similarity of that feature between normal cells and perturbed cells.

The measure of similarity can be either a standard statistical measure such as the Kolmogorov-Smirnov (KS) test [30], the  $z$ -test [25], the  $t$ -test [25], the  $\chi^2$ -test [6], or it can be a machine-learning based technique such as the neural networks [2], Support Vector Machine (SVM) [31], Random Forest [28], etc.

Then, the methodology to deal with the “off-target-effects” is applied to the phenotypic vectors coming from each RNA molecule.

A classical method is based on RNA selection. It consists of using multiple RNA molecules targeting the same gene, and keeping only the common phenotypic perturbations. Echeverri *et al.* [8] stated that if at least 2 out of 3 used RNA molecules produce the same phenotype changes, we can consider it as “on target”. In addition, they recommend to repeat the experiment to validate the results.

An alternative method consists of making an average gene profile. In that case, using again several RNA molecules targeting the same gene, one averages the multiple resulting vector of phenotypic measurements. Collinet *et al.* [6] compute the most probable phenotype using a Bayesian model.

### 1.3 Our contributions

We first propose in section 4 a model based on a Vector Quantization [14, 23]. Using the  $K$ -means algorithm, we find clusters in the feature space, and use a hard classification rule to determine whether samples in a cluster are “on-target” components, or “off-target” components (section 4.1). In section 4.2, we propose a soft version of this classification rule using a probabilistic  $K$ -means. Note that choosing the optimal number of clusters is not straightforward. In the context of unsupervised learning, some methods assess the optimal number of clusters [19, 20]. These methods start with an empty set of clusters which is filled dynamically using on line learning. In unsupervised learning, the objective is to model the sample distribution. By contrast, we tackle the special case of supervised clustering. We do not want to model the sample distribution, we rather want a model of the class specificities and of the class mixtures. In this context, assessing the number of clusters is different from unsupervised techniques [19, 20]. We address the supervised selection of the cluster number in section 4.3.

Our second contribution, presented in section 5, is based on the analysis of the Random Forest outputs [5, 4]. We start from the idea that the “RNA entropy” of an on-target component – that is the entropy of the distribution of the RNA used to produce the phenotypes in that cluster – is high, since multiple RNA molecules are represented. Conversely, an off-target component resulting from a single RNA molecule leads to a small RNA entropy. In order to compute this entropy, each sample is associated to a probability vector that is build from tree-based classification steps.

In addition, we propose to use the two methods above as a mean to initialize the Expectation-Maximization (EM) procedure. Collinet *et al.* [6] proposed a Gaussian mixture model to characterize the “on-target” component, but the parameters of the model are trained from an EM algorithm which is very sensitive to its initialization. We show that our approach drastically improves the recognition performance. The Gaussian mixture model being our baseline, this is the first methodological approach we present, see section 3.

### 1.4 Data sets

In section 6.1, in order to interpret the results, we use a synthetic 2D data set.

Both section 6.2 and section 6.3 consider an application in the field of neuroscience. We propose to characterize cells’ development dynamics in time-laps movies [17]. In the field of neurobiology, it has been observed connections between the static morphological properties of a cell and its genotype [27]. More recent works in oncology have shown that studying the cell growth dynamics provides important information about the cell genotype [11, 24]. Following that line of thinking, biologists want to quantify how much neurites’ morphodynamic depends on the genotype characteristics.

For instance, Figure 1-(a) shows one video of neurons for which the gene RhoA has been inhibited, which leads to longer neurites. Figure 1-(b) shows one video of neurons for which the gene Map2K7 has been inhibited which leads to shorter neurites and faster protrusion and retraction process.

The characterization of such aspects of the neurite phenotypes, requires to deal with the “off-target-effect”, which is our core objective.

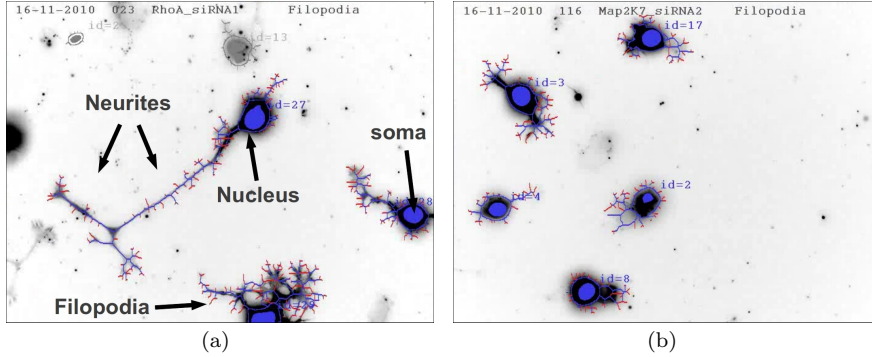


**Fig. 1** (a) A video that contains some cells for which the gene RhoA is inhibited. This leads to bigger neurites. (b) A video that contains some cells for which the gene Map2K7 is inhibited. This leads to shorter neurites.

## 2 Basic idea

Before we deal with the methodological and experimental aspects, we present the concepts and the basic idea of the process and introduce notation.

We consider that a cell is represented by a set of  $F$  features: the soma area, the instantaneous soma speed, the number of neurites, the neurite total length, the instantaneous neurite activity (protruding or retracting), *etc.* Let  $X \in \mathbb{R}^F$  be the feature vector associated to a cell.

We consider  $M$  RNA molecules that inhibit the same gene, to which correspond  $M$  cell classes. We consider  $M+1$  distributions for  $X$ , one corresponding to the “on-target” component, and the  $M$  others to the “off-target” components.

This is illustrated in figure 2. We consider a synthetic example with three RNA molecules ( $M = 3$ ), and where each cell is represented by two features ( $F = 2$ ): its speed and its size. Each cell is represented by a vector in the two-dimensional feature space. These vectors are depicted by crosses, dots and squares, depending on the RNA molecule which is associated with each cell. We identify four clusters ( $M+1 = 4$ ). The first cluster is the “on-target” component which is composed of every RNA molecules. The three other clusters are the “off-target” components that are composed of a single RNA molecule each.

The methods we propose aim at characterizing the statistical distribution of each cluster. Then, we can remove the “off-target” components and we are able to extract the phenotypic gene profile. This approach assumes two important properties: (a) the “off-target” components and the “on-target” component are additive in the feature space, and (b) at least one RNA molecule must be absent in each of the “off-target” components.

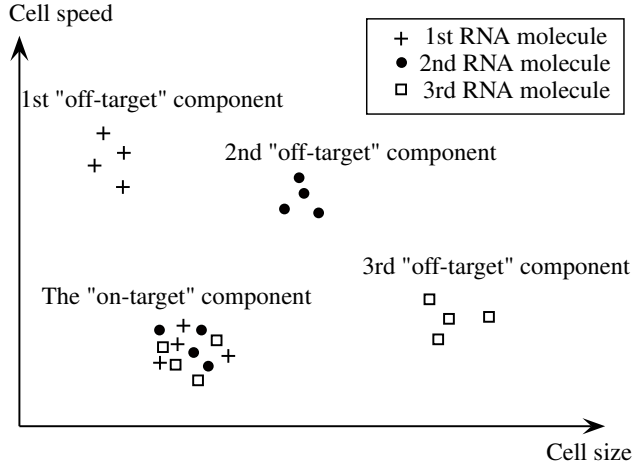


**Fig. 2** In this schematic example, we consider that a cell is described by two features ( $F = 2$ ): its speed and its size. In the figure, a cell is represented by a vector in the two-dimensional feature space. There are three RNA molecules ( $M = 3$ ) that are represented by crosses, dots, and squares, respectively. The “Off-target” components are represented by the clusters that contain vectors from single RNA molecules. The “On-target” component is the cluster that contains vectors from every RNA molecules.

### 3 Gaussian Mixture Model (GMM)

In order to understand the baseline [6], we introduce the Gaussian mixture model and the Expectation-Maximization training procedure. For a random initialization, the method is called “Random+GMM”, else, by using an other initialization that we call “*init*”, the method is designated as “*init+GMM*”.

#### 3.1 State-of-the-art

Gaussian-Mixture models (GMM) are mostly used to model a statistical distribution of vectors. The distribution  $g$  of the random variable  $X \in \mathbb{R}^F$  has the following form:

$$g(x) = \sum_{c=1}^C \rho_c \mathcal{N}(x | \mu_c, \Sigma_c) \quad (1)$$

where  $C$  denotes the number of components in the mixture,  $\mathcal{N}(X \mid \mu_c, \Sigma_c)$  denotes the multivariate normal distribution with mean  $\mu_c$  and covariance matrix  $\Sigma_c$ , and  $\rho_c$  denotes the component prior.

Dempster *et al.* [7] proposed to assess the parameters  $\Theta = \{\rho_c, \mu_c, \Sigma_c\}_{c=1}^C$  with an Expectation-Maximization (EM) algorithm [7]. If we consider a diagonal covariance matrix,  $K$ -means [10] is also suitable.

The model can be extended to a classification task where each class is independently modeled using equation (1). Let  $M$  be the number of classes, and  $g_t$  be the class  $t$  distribution. The distribution  $f$  of a random variable  $X \in \mathbb{R}^F$  has the following expression:

$$f(x) = \sum_{t=1}^M \pi_t g_t(x) \quad (2)$$

In supervised learning, the parameters  $\{\pi_t, \Theta_t\}_{t=1}^M$  are learned independently, class by class, by using the usual EM procedure [7], where  $\Theta_t$  are the parameters of  $g_t$ . Note that the training data set  $\{X_n, Y_n\}_{n=1}^N$  is composed of the vectors  $X_n \in \mathbb{R}^F$  and the labels  $Y_n \in \{1, \dots, M\}$ .

In weakly supervised learning, the label  $Y_n$  is a hidden variable. The training data set is  $\{X_n, \pi_n\}_{n=1}^N$ , where  $\pi_n = \{\pi_{n,t}\}_{t=1}^M$  is a vector that indicates the prior probability that sample  $X_n$  belong to each class:

$$\pi_{n,t} = p(Y_n = t) \quad (3)$$

In the case of equi-probable prior  $\pi_{n,t} \in \{0, 1/M\}$ , Bishop and Ulusoy [3] proposed an EM approach to train the parameters  $\{\pi_t, \Theta_t\}_{t=1}^M$ . This method has been extended to any prior value  $\pi_{n,t} \in [0, 1]$  in [16].

At iteration  $(i)$ , given a training data set  $\{X_n, \pi_n\}_{n=1}^N$  and the current values of the parameters for class  $t$

$$\Theta_t^{(i)} = \left\{ \rho_{t,c}^{(i)}, \mu_{t,c}^{(i)}, \Sigma_{t,c}^{(i)} \right\}_{c=1}^C,$$

the EM procedure consists of: In the first step, which is called the “expectation” step, we compute for each sample both the class posterior:

$$\gamma_{n,t} = \frac{\pi_{n,t} g_t^{(i)}(X_n)}{f^{(i)}(X_n)} \quad (4)$$

and the component posterior:

$$\alpha_{n,t,c} = \frac{\rho_{t,c} \mathcal{N}(X_n \mid \mu_c^{(i)}, \Sigma_c^{(i)})}{g^{(i)}(X_n)} \quad (5)$$

In the second step, which is called the “maximization” step, we update the new set of parameters  $\Theta_t^{(i+1)}$ :

$$\rho_{t,c}^{(i+1)} = \frac{\sum_{n=1}^N \gamma_{n,t} \alpha_{n,t,c}}{\sum_{n=1}^N \gamma_{n,t}} \quad (6)$$

$$\mu_{t,c}^{(i+1)} = \frac{\sum_{n=1}^N \gamma_{n,t} \alpha_{n,t,c} X_n}{\sum_{n=1}^N \gamma_{n,t} \alpha_{n,t,c}} \quad (7)$$

$$\Sigma_{t,c}^{(i+1)} = \frac{\sum_{n=1}^N \gamma_{n,t} \alpha_{n,t,c} (X_n - \mu_{t,c}^{(i+1)}) (X_n - \mu_{t,c}^{(i+1)})^T}{\sum_{n=1}^N \gamma_{n,t} \alpha_{n,t,c}} \quad (8)$$

These two steps are iterated until convergence. We consider that the method converges when the likelihood is stabilized. The number of components  $C$  per mixture is assessed by maximizing the likelihood, or by using the Mean-Shift algorithm [32]. In this paper, we maximize the likelihood to learn the parameters.

### 3.2 Modeling the RNA perturbations with GMM

Following section 2, we consider cells represented by vectors  $\{X_n^m\}_{n=1}^{N_m}$ , where  $X_n^m \in \mathbb{R}^F$  represents a cell which is obtained from the RNA molecule  $m \in \{1, \dots, M\}$ .

Ideally, if there was no “off-target-effect”, these vectors would all follow the same distribution  $g_0$  that we call the “on-target” component. However, in practice, there is an “off-target” component following the distribution  $g_m$ . In this situation, a vector  $X_n^m$  is generated by either  $g_0$  or  $g_m$ , and its distribution is a mixture of the “on-target” component  $g_0$  and the specific “off-target” component  $g_m$ . Let  $f_m$  be that mixture distribution. Then, the relation between  $\{f_m\}_{m=1}^M$  and  $\{g_t\}_{t=0}^M$  is as follows:

$$f_m = \pi_0^m g_0 + (1 - \pi_0^m) g_m, \quad (9)$$

where  $\pi_0^m \in [0, 1]$  is the prior probability that a vector is generated by the “on-target” component. By considering all the RNA molecules, the distribution takes the following expression:

$$f = \sum_{m=0}^M (1 - \pi_0^m) g_m \quad (10)$$

where  $1 - \pi_0^0 = \sum_{m=1}^M \pi_0^m$ . The model (10) being the same as the model (2), we can consider the EM algorithm [16] to train the parameters  $\{\Theta_t\}_{t=0}^M$ .

In this application, we can also include some specific constraints. Let  $Y_n^m$  be a random variable on  $\{0, \dots, M\}$  which specifies which component generated  $X_n^m$ . If  $Y_n^m = 0$ , sample  $X_n^m$  is generated by the “on-target” component  $g_0$ , and  $\forall t > 0$  if  $Y_n^m = t$ , sample  $X_n^m$  is generated by the “off-target” component

$g_t$ . Since we know which RNA molecule is associated to each cell, we have the following rules:

$$\begin{cases} p(Y_n^m = t) = 0 & \text{if } t > 0, t \neq m \\ p(Y_n^m = 0) = \pi_0^m \\ p(Y_n^m = m) = 1 - \pi_0^m \end{cases} \quad (11)$$

In other words, a cell obtained from a RNA molecule  $m$  can not be generated from an “off-target” component of an other RNA molecule  $t \neq m$ . It is generated by either the “on-target” component, or the “off-target” component of the considered RNA molecule  $m$ . Then, from the constraints (11), we define the new posteriors at the current iteration ( $i$ ):

$$\begin{cases} \gamma_{n,t}^m = 0 & \text{if } t \neq m \\ \gamma_{n,t}^m = \frac{\pi_0^m g_0^{(i)}(X_n^m)}{f_m^{(i)}(X_n^m)} & \text{if } t = 0 \\ \gamma_{n,t}^m = \frac{(1 - \pi_0^m) g_m^{(i)}(X_n^m)}{f_m^{(i)}(X_n^m)} & \text{if } t = m \end{cases} \quad (12)$$

This method allows to characterize each component of the distribution of the random variable  $X_n^m$ . We can now classify the vector  $X_n^m$  as being “on-target” or “off-target”. This classification step is achieved by using the Bayes rule:

$$\begin{cases} p(Y_n^m = 0 | X_n^m, \Theta_0, \dots, \Theta_M) = \frac{\pi_0^m g_0(X_n^m)}{f_m(X_n^m)} \\ p(Y_n^m = m | X_n^m, \Theta_0, \dots, \Theta_M) = \frac{(1 - \pi_0^m) g_m(X_n^m)}{f_m(X_n^m)} \end{cases} \quad (13)$$

### 3.3 Estimation of the parameters

The first parameter to set is the number of iterations of the EM algorithm. We stop the iterations when the likelihood  $\mathcal{L}(\{X_n^m\}, \{\Theta_t^{(i)}\})$  at iteration  $i$  is very close to the likelihood at iteration  $i + 1$ . In other words, we stop the iteration whether:

$$\left| \mathcal{L}(\{X_n^m\}, \{\Theta_t^{(i+1)}\}) - \mathcal{L}(\{X_n^m\}, \{\Theta_t^{(i)}\}) \right| < \epsilon \quad (14)$$

In practice, using our dataset, we noticed that the classification performances do not change after 50 iterations. So, the number of iterations is set to 50. But, if a user does not know a dataset, we recommend to train  $\epsilon$  by grid search.

The second parameter to set is  $C$ , i.e. the targeted number of components per class (see equation (1)). The parameter is optimized by using a grid search. We choose the optimal value  $C \in \{2, 4, 16, 32, 64, 128\}$  that maximizes the likelihood:

$$\hat{C} = \arg \max_C \mathcal{L}(\{X_n^m\}, \{\Theta_t\}, C) \quad (15)$$

Note that for our classification task, we do not need a fine evaluation of the number of Gaussian components per class. This value can even be overestimated to guarantee a proper assessment of the "off-target-effect". The cell classification being more important than a good model distribution, we set a rough grid for  $C$ .

There is no prior on the data. Hence, at the initialization step, it is reasonable to give the same weight to both the "off-target-effect" and the "on-target-effect". As a consequence, each effect has the same probability to appear. So, the priors  $\{\pi_0^t\}_{t=0}^M$  are set to 0.5 at the beginning of the EM algorithm.

## 4 Vector Quantization

We investigate in this section an alternative approach to the discovery of the "off-target" effect, which bypass the modeling of the respective distributions, and directly attempts at classifying each sample as either "off-target" or "on-target".

### 4.1 A hard classification rule (hard-VQ)

This method relies on the analysis of the presence or the absence of the RNA molecules in each region of the feature space. These regions are build using a vector quantization algorithm. If all the RNA molecules are present in a region of the feature space, we assume that these cells are generated from the "on-target" component. If a RNA molecule is not present in a region of the feature space, we further assume that this region is "off-target". This is illustrated in Figure 2: the "off-target" components contain only crosses, dots, or squares, while the "on-target" component contains all of the crosses, the dots, and the squares. We call this method "hard-VQ".

Formally, let  $\{X_n^m\}_{n=1}^{N_m}$  be a representation of the cells in the feature space, where the vector  $X_n^m \in \mathbb{R}^F$  represents a cell which is obtained from the RNA molecule indexed by  $m \in \{1, \dots, M\}$ . The first step of the method consists of dividing the feature space into  $K$  clusters. This is achieved by using the  $K$ -means algorithm [10] from all the available vectors  $\{\{X_n^m\}_{n=1}^{N_m}\}_{m=1}^M$ . Let

$$I_n^m \in \{1, \dots, K\}$$

be the index of the cluster which is associated to the sample  $X_n^m$ , and let

$$H_k = \{H_k^m\}_{m=1}^M$$

be the histogram that of the vector distribution of the  $M$  RNA molecules in cluster  $k \in \{1, \dots, K\}$ . Each component  $H_k^m$  of the histogram  $H_k$  takes the

following formal expression:

$$H_k^m = \frac{\sum_{n=1}^{N_m} \mathbb{1}_{\{I_n^m=k\}}}{\sum_{j=1}^M \sum_{n=1}^{N_j} \mathbb{1}_{\{I_n^j=k\}}} \quad (16)$$

where  $\mathbb{1}_{\{I_n^m=k\}} = 1$  if  $I_n^m = k$ , and  $\mathbb{1}_{\{I_n^m=k\}} = 0$  otherwise.

The second step of the method consists of classifying each cluster into either “off-target” or “on-target”. To this end, we analyze the histograms  $\{H_k\}_{k=1}^K$ . Let  $d(k) \in \{0, 1\}$  be the classification result, i.e. the decision, where  $d(k) = 1$  if the  $k$ th cluster is considered as “on-target”, and  $d(k) = 0$ , if the  $k$ th cluster is considered as “off-target”. The classification rule is defined as follows:

$$d(k) = \mathbb{1}_{\{\forall m, H_k^m > 0\}} \quad (17)$$

In other words, if all the RNA molecules are present in the  $k$ th cluster, all the components of the vector  $H_k$  are different from zero, then, this cluster is considered as an “on-target” component. If there is at least one RNA molecule which is absent in the  $k$ th cluster, there is at least one component of the vector  $H_k$  which equals to zero, then we consider this cluster as an “off-target” component.

Finally, we define the RNA class posterior  $p(Y_n^m | X_n^m, H_1, \dots, H_K)$ , where  $Y_n^m$  is defined in section 3 from the decision rule (17), with

$$\begin{cases} p(Y_n^m = t | X_n^m, H_1, \dots, H_K) = 0 \text{ if } t > 0, t \neq m, \\ p(Y_n^m = 0 | X_n^m, H_1, \dots, H_K) = \mathbb{1}_{\{d(I_n^m)=1\}}, \\ p(Y_n^m = m | X_n^m, H_1, \dots, H_K) = \mathbb{1}_{\{d(I_n^m)=0\}}. \end{cases} \quad (18)$$

In other words, if the vector  $X_n^m$  is in a cluster classified as “on-target”, we set  $Y_n^m = 0$ , and if the vector  $X_n^m$  is in a cluster classified as “off-target”, we set  $Y_n^m = m$ .

Note that in this paper, the  $K$ -means procedure is initialized using the  $K$ -means++ algorithm [1].

#### 4.2 A soft version of the classification rule (soft-VQ)

We propose to extend the hard classification rule (18) to a soft version, by using a probabilistic version of the  $K$ -means. This method is called “soft-VQ”. The idea is to generate several clusterings and to merge them together. By doing this, we aim to reduce the influence of the  $K$ -means initialization, and then, we expect to improve the recognition performance. The main reason of that improvement comes from the reduction of the noise brought by the vectors that are close to the cluster boundaries.

The algorithm is based on bootstrapping. We want to combine  $B$  classifiers. At step  $b \in \{1, \dots, B\}$ , in order to build a classifier, we apply the  $K$ -means algorithm on a random sub-population of the training data. This sub-population is composed of vectors which are sampled at random among  $\{\{X_n^m\}_{n=1}^{N_m}\}_{m=1}^M$ . The proportion of sampled training data is denoted by  $\alpha$ . Using the classification rule (17), we classify the clusters at step  $b$  into “on-target” component or “off-target” component. Following the “Bagging” idea [4], the final decision to classify  $X_n^m$  as being either an “on-target” component or an “off-target” component is taken from a vote.

Formally, let  $d^b(k) \in \{0, 1\}$  be the decision taken by the classifier at step  $b$ , where  $d^b(k) = 1$  if the  $k$ th cluster is considered as “on-target”, and  $d^b(k) = 0$ , if the  $k$ th cluster is considered as “off-target”. Then, the posterior takes the formal expression:

$$\begin{cases} p(Y_n^m = 0 | X_n^m, H_1, \dots, H_K) = \frac{1}{B} \sum_{b=1}^B \mathbb{1}_{\{d^b(I_n^m) = 1\}} \\ p(Y_n^m = m | X_n^m, H_1, \dots, H_K) = \frac{1}{B} \sum_{b=1}^B \mathbb{1}_{\{d^b(I_n^m) = 0\}} \end{cases} \quad (19)$$

Note that in this paper, we set the number of  $K$ -means to  $B = 100$  and the proportion of random training data to  $\alpha = 0.5$ .

#### 4.3 Estimation of $K$

Setting  $K$  is very important and not straightforward. If  $K$  is too high, all the clusters may contain only one type of RNA molecule. In that case, all the samples may be considered to be “off-target”. On the other hand, if  $K$  is too small, we can expect that all the RNA molecules are present in each cluster. In that case, all the cells will be considered to be “on-target”. In order to address this issue, we propose an optimization criterion which forces the vector distributions of the “on-target” components to be similar and the vector distributions of the “off-target” components to be different.

Let  $\{X_n, Y_n\}_{n=1}^N$  be the training data set, where  $X_n \in \mathbb{R}^F$  is a cell and  $Y_n \in \{1, \dots, M\}$  indicates the index of the RNA molecule. From either the posterior (18) or the posterior (19), we derive the decision rule  $d_n(K)$  which is similar to the decision (17). If  $X_n$  is considered to be on target,  $d_n(K) = 0$ . Else, if  $X_n$  is considered to be off target,  $d_n(K) = 1$ . We want a value of  $K$  that both minimizes the distance between the “on-target” distributions and maximizes the distance between the “off-target” distributions.

To achieve this, the optimal value of  $K$  is defined as:

$$\hat{K} = \arg \max_K [\Delta_1(K) - \Delta_0(K)] \quad (20)$$

where

$$\Delta_t(K) = \sum_{m_1 \neq m_2} \delta [\mu_t^{m_1}(K), \mu_t^{m_2}(K)]$$

is an average distance and  $\mu_t^m(K) \in [0, 1]^{K'}$  denotes a model of the distribution  $\{X_n \mid Y_n = m, d_n(K) = t\}$ . The distribution function  $\mu_t^m(K)$  is computed using the bag-of-word model [18]. In other word,  $\mu_t^m(K)$  is a histogram that counts the number of samples in  $\{X_n \mid Y_n = m, d_n(K) = t\}$  that are in each of  $K'$  clusters. The  $K'$  clusters are computed using a  $K$ -means. The Bhattacharyya distance is used to compute the distance:

$$\delta[\mu_t^{m_1}(K), \mu_t^{m_2}(K)] = 1 - \sum_{k=1}^{K'} \sqrt{\mu_{t,k}^{m_1}(K) \mu_{t,k}^{m_2}(K)} \quad (21)$$

For a given set of values  $K \in \{K_1, \dots, K_Q\}$ , we noticed that the value ranges of  $\Delta_1(K)$  and  $\Delta_0(K)$  are different. In order to have the same dynamics for both distance measures, the measures are normalized as follows:

$$\Delta_t(K) \leftarrow \frac{\Delta_t(K) - \min\{\Delta_t(K)\}_{K=K_1}^{K_Q}}{\max\{\Delta_t(K)\}_{K=K_1}^{K_Q}} \quad (22)$$

This normalization forces the distance measures in the range from 0 to 1.

In this paper, the optimization criterion (20) is solved using a grid search where  $K \in \{2^q\}_{q=2}^{12}$ , and the number of clusters for the bag-of-words model is set to  $K' = 1024$  (see equation (21)).

## 5 Random forest

Our last method is based on bagging and Random Forests [9, 4, 15]. We train a bag of decision trees to predict the RNA molecule associated to a certain phenotypical vector, and we estimate how the said molecule can be predicted from the phenotype using the posterior entropy. We will refer to this method as “forest”.

The idea is that if a cell is “on-target”, it is difficult to know from which RNA molecule it is from, since all the RNA molecules are present in an “on-target” component. Thus, if we try to classify the cells among the RNA molecules, the classification error rates of the “on-target” cells will be high. The RNA entropy which characterizes the RNA probability will also be high.

On the other hand, given a set of cells that are “off-target”, it is reasonable to suppose that the cell classification error will be low since an “off-target” component contains less RNA molecules than an “on-target” component. Thus, in the case of an “off-target” component, the RNA entropy is low.

From these properties, we can derive an entropy-based index to characterize the level of RNA uncertainty and to know whether a cell is either “on-target” or “off-target”. In the next part of this section, we formulate the problem in a formal way.

Let  $B$  be the number of trees in the forest. In order to train a tree  $f_b$  of the forest, the data set  $\{X_n, Y_n\}_{n=1}^N$  is split randomly into a train set and a test set,

where  $X_n \in \mathbb{R}$  is a cell and  $Y_n \in \{1, \dots, M\}$  is the index of the RNA molecule. Then, for a given test sample  $X$ , we can assign a class  $f_b(X) \in \{1, \dots, M\}$ . From the forest, we compute the class probabilities  $\gamma_n = \{\gamma_{n,1}, \dots, \gamma_{n,M}\}$ , where  $\gamma_{n,m} \in [0, 1]$  and  $\sum_{m=1}^M \gamma_{n,m} = 1$ . Formally,  $\gamma_{n,m}$  is related to the occurrence of each class:

$$\gamma_{n,m} = \frac{1}{B} |\{b \text{ s.t. } f_b(X_n) = m\}| \quad (23)$$

From the probability vector  $\gamma_n$ , we propose an entropy-based rule to decide whether  $X_n$  is “on-target” or “off-target”. The entropy  $h_n$  allows characterizing the homogeneity of the vector  $\gamma_n$ :

$$h_n = - \sum_{m=1}^M \gamma_{n,m} \log \gamma_{n,m}$$

We propose the following rule:

$$\begin{cases} \text{if } h_n > \frac{1}{N} \sum_{n'=1}^N h_{n'}, X_n \text{ is “on-target”} \\ \text{if } h_n < \frac{1}{N} \sum_{n'=1}^N h_{n'}, X_n \text{ is “off-target”} \end{cases} \quad (24)$$

More intuitively, if  $h_n$  is low,  $X_n$  is always classified in the same class, which means that it is from an “off-target” component. While if  $h_n$  is high,  $X_n$  is classified among each of the RNA molecule, which means that it is from a “on-target” component. In addition, because we know that an “on-target” component is composed of all the classes, we consider the following constraint that if:

$$\prod_{m=1}^M \gamma_{n,m} = 0 \quad (25)$$

the vector  $X_n$  is considered as “off-target”.

In this paper, the trees are trained using the CART algorithm [5] and we set the number of trees in the forest to  $B = 100$ . In addition, the proportion between the random training data and the random test data to  $\alpha = 0.5$ .

## 6 Experiments

### 6.1 Toy examples

In this section, a subjective analysis is suggested to show that the proposed methods are able to distinguish the “off-target” components from the “on-target” component. In this way, we generate a random data set that is visually easy to interpret in a 2D feature space. Both the “on-target” component and

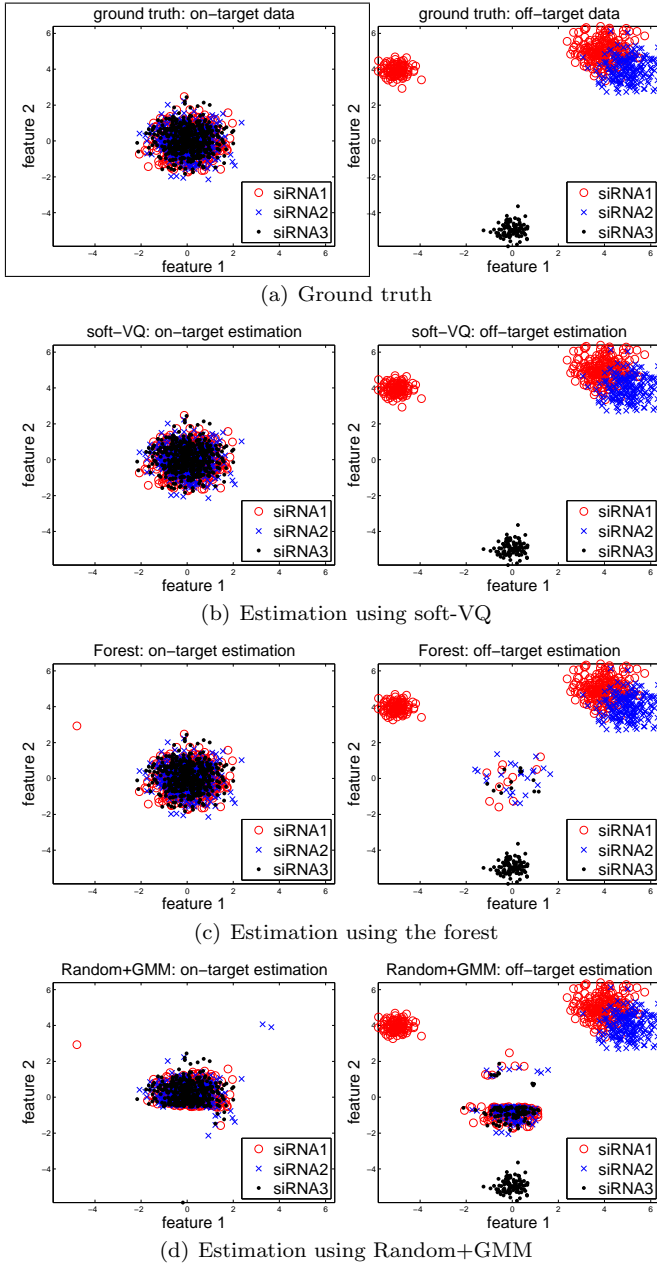


**Fig. 3** Subjective analysis from a toy synthetic data set. (a) The ground truth. (b) Estimation using a soft Vector Quantization (soft-VQ). (c) Estimation using a random forest (Forest). (d) Estimation using a Gaussian mixture model (Random+GMM).

the “off-target” components follow Gaussian distributions, such that the means and the variances are chosen arbitrarily.

The results are given in Figure 3. Figure 3-a shows the raw data, i.e. the data as they are generated. Figure 3-b shows the classification results for soft-VQ (section 4). Figure 3-c shows the classification results for the random forest (section 5). Figure 3-d shows the classification results for the GMM (section 3).

The similarity between the estimated components in Figure 3-b and the ground truth in Figure 3-a shows that the method soft-VQ is able in that case to recognize the “off-target” components. The forest and the GMM [6] filtered a lots of the “off-target” vectors as well, but are less precise.

## 6.2 Semi-synthetic data set

The subjective analysis in section 6.1 is used to illustrate the issue and the kinds of results we obtain. But, a robust quantitative analysis must be carried out to compare the methods using real data. We use cells in time laps movies (Figure 1).

Initially, each cell is represented by 240 features. Some features characterize both the soma and nucleus shapes in each frame: Position, area, eccentricity, major axis length, minor axis length, perimeter, and circularity. We also characterize the distribution of these values in a video by using the quantiles  $\{0, 0.25, 0.5, 0.75, 1\}$ . In addition, we compute the dynamical version of these static measures by computing the Euclidean distance between the feature values in two consecutive frames. For instance, the instantaneous speed is the dynamical version of the position. To be more exhaustive, we add both the instantaneous acceleration, and the distance traveled, and we compute their distributions in the video by using the quantiles.

Then, for all the static features, we compute the frequency of the protrusion-retraction process, i.e. the number of times a soma is growing or retracting. Other features characterize a neurite in each frame: number of branches, number of leaves, distribution of the branch lengths (using the quantiles), the extreme length (the longest path from the root to a leaf), the total cable length, and the neurite complexity that equals the extreme length divided by the number of branches. Again, in order to have a neuron-based measure, we characterize their distribution by using the quantiles. We also characterize the neurite feature distribution in a video by using the quantiles. In addition, the instantaneous number of neurites is computed as well as its distribution in the video. Then, we compute the frequency of the protrusion-retraction process, i.e. the number of times a neurite is growing or retracting.

Finally, some features characterize the change between two images in the video. They are based on the entropy or they are pixel-based. Their distribution is computed by using the quantiles.

In order to reduce the complexity, we select the 20 best features by using the Kolmogorov-Smirnov test[30], which leads to a vector of 20 components for each cell.

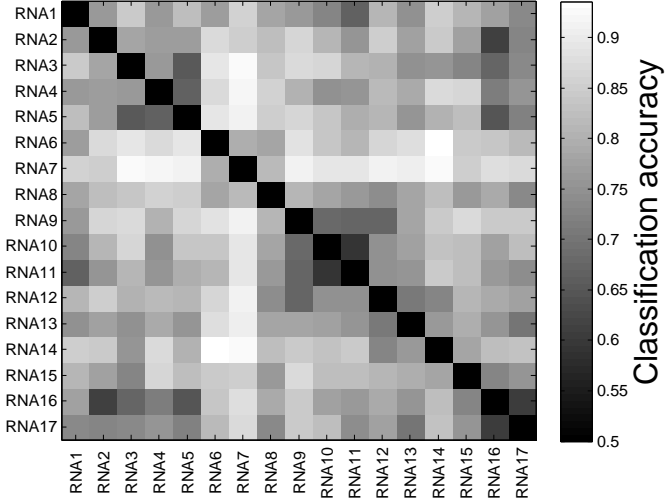


**Fig. 4** Measure of the phenotypic distance between each RNA molecule. The higher the classification accuracy the higher the distance.

Because of the many possible cell phenotypes, it is not straightforward to have an annotated data set. That is why we built a semi-synthetic data set from a set of 17 RNA molecules. To do this, we first evaluate the phenotypic distance by using the classification accuracy as measure of the distance. The classification accuracy is computed from 100 cross validation steps by using a Support Vector Machine with a Gaussian kernel [29]. Second, using the distance matrix that is given in Figure 4, we choose the  $M+1$  RNA molecules that are the most further apart from each other. Then, one of the RNA molecule is chosen at random to be the “on-target” component, and the remaining RNA molecules are associated to each of the  $M$  RNA “off-target” components. By doing this, we build a data set which ensures both the “on-target” and the “off-target” components to have different distributions, while making these distributions realistic. In order to statistically characterize the recognition performance and to identify the best method, this random procedure is repeated 100 times. At the end, we compute a mean correct classification accuracy, that is the average between the correct classification rate of the “on-target” class and the correct classification rate of the “off-target” class. The standard deviation is also computed to indicate the unstable methods.

All the results are given in Table 1. For each method, we plot the classification accuracy as a function of  $M$ , the number of RNA molecules. We note

only compare the GMM (section 3), the hard-VQ (section 4.1), the soft-VQ (section 4.2), and the forest (section 5), we also initialize the GMM by using hard-VQ, soft-VQ, and the forest. The method “Random” is a random classification that provides a lower bound.

**Table 1** Recognition performances as a function of the number of virtual RNA molecules. The reported value represents the mean correct classification rate.

Number of RNA molecules	$M = 2$	$M = 3$	$M = 4$	$M = 5$
hard-VQ	0.70±0.13	0.65±0.17	0.62±0.17	0.61±0.17
hard-VQ+GMM	0.71±0.11	0.70±0.09	0.68±0.09	0.64±0.10
soft-VQ	0.73±0.11	0.70±0.21	0.63±0.18	0.63±0.17
soft-VQ+GMM	0.73±0.12	<b>0.73±0.10</b>	<b>0.69±0.10</b>	<b>0.66±0.09</b>
Forest	<b>0.77±0.06</b>	<b>0.73±0.05</b>	<b>0.69±0.06</b>	0.64±0.09
Forest+GMM	0.73±0.08	0.68±0.06	0.65±0.05	0.61±0.04
Random	0.37±0.06	0.33±0.04	0.31±0.03	0.30±0.03
Random+GMM	0.51±0.05	0.50±0.04	0.50±0.04	0.50±0.03

From these results, we can make several observations. First of all, soft-VQ and the forest outperform the other methods. Second, in comparison to the GMM [6], we drastically improve the recognition performance by using the proposed methods or by initializing the GMM with the proposed methods. This improvement goes from about 10% to about 25% in the best case. Also, the probabilistic  $K$ -means we proposed (soft-VQ) outperforms the hard decision rule (hard-VQ) with a range from 1% to 5%. In addition, these results point out that the EM algorithm needs a proper initialization. For instance, there is a 23% improvement by initializing the GMM with the soft-VQ ( $M = 2$  and  $M = 3$ ). To be done with the observations, we notice that the VQ-based methods have a standard deviation which is about 15, while it is about 5 for the forest and the GMM. Thus, in comparison to soft-VQ, soft-VQ+GMM allows both improving the recognition performance and reducing the instability.

### 6.3 Real data set

In collaboration with biologists, we manually annotated a data set. We want to characterize the neurite outgrowth of the cells in time laps movies (Figure 1). A neurite is represented by three features: the total cable length of the neurite, the extreme length of the neurite, and the number of branches in the neurite. We have two sets of movies: cells for which the gene HGS is knockdown and cells for which the gene TRAF2 is knockdown. For each of these two set of

movies, there are three sub-set of movies, each sub-set being related to a RNA molecule.

In order to annotate the data, we use the following protocol. For each possible pair of features, we plot the data in the 2D feature space, and then, we manually designate the off-target vectors. The annotation result is shown in Figure 5-a for the gene HGS and in Figure 6-a for the gene TRAF2. The three RNA molecules are respectively represented by red circles, blue crosses, and black dots. As waited, the “on-target” component contains cells from the three RNA molecules, while the “off-target” component contains cells from either one or two RNA molecules. Figure 5-b and Figure 6-b show the classification results by using the soft-VQ model. This subjective analysis demonstrates that we properly identify the different components.

**Table 2** Classification accuracy for the genes TRAF2 and HGS. The reported value represents the mean correct classification rate.

Gene names	HGS	TRAF2
hard-VQ	0.94	0.91
hard-VQ+GMM	0.80	0.84
soft-VQ	<b>0.96</b>	<b>0.94</b>
soft-VQ+GMM	0.83	0.81
Forest	0.76	0.80
Forest+GMM	0.78	0.83
Random	0.25	0.25
Random+GMM	0.70	0.76

In order to quantify the error rate, we provide the classification accuracy as well. The recognition performances are given in Table 2 for each of the methods. As previously, our proposed methods allow improving drastically the classification accuracy in comparison to the GMM baseline [6] in a range from 8% to 26%. In addition, our proposed methods are better for the GMM initialization than a random GMM initialization (about 10%). In comparison to section 6.2, the VQ-based methods clearly outperform the forest. This is due to the default values of the forest parameters (number of trees and training proportion) that are not fitted to this new data set. The advantage of the VQ-based methods is that we estimate the optimal number of clusters (section 4.3).

Note that these results mainly depend on the quality of the data annotation. The fact that we obtain more than 90% of classification accuracy proves that the annotation procedure has been well designed.

In Table 3, we report an analysis of the main parameter sensitivity. The four main parameters are the bootstrapping parameters ( $B$  and  $\alpha$ ) that are used for both Forest and soft-VQ. We characterize their sensitivity by com-

puting the average standard deviation of the classification accuracy. If the standard deviation is high, the dispersion of the classification accuracy is high. Regarding the parameter  $B$ , we note that the accuracy dispersion is lower if  $B \in \{100, 200, 300, 400, 500\}$ . This means that it is equivalent to use  $B = 100$  and  $B = 500$ . In addition, we note that the classification performance increases from  $B = 1$  to  $B = 100$  and becomes steady from  $B = 100$ . For this reason, we use  $B = 100$ . Regarding the parameter  $\alpha$ , we note that the dispersion always increases when we remove the extreme values of *alpha* (either  $\alpha = 0.1$  or  $\alpha = 0.9$ ). As a consequence, setting  $\alpha = 0.5$  is a good compromise that ensures a better choice than random.

**Table 3** In this table, we report an analysis of the sensitivity of the two main parameters  $B$  and  $\alpha$  that define the bootstrapping environment of both Forest and soft-VQ. We report the average standard deviation of the classification accuracy. In order to study the sensitivity of the parameter  $B$ , we compute the standard deviation of the classification accuracy for each value of  $\alpha$  given a value of  $B$ , then we average the standard deviation. In order to study the sensitivity of the parameter  $\alpha$ , we compute the standard deviation of the classification accuracy for each value of  $B$  given a value of  $\alpha$ , then we average the standard deviation. Let  $B_1 = \{10, 50, 75, 100, 200, 300, 400, 500\}$ ,  $B_2 = \{100, 200, 300, 400, 500\}$ ,  $\alpha_1 = \{0.1, 0.3, 0.5, 0.7, 0.9\}$ ,  $\alpha_2 = \{0.3, 0.5, 0.7\}$ ,  $\alpha_3 = \{0.1, 0.3, 0.5\}$ , and  $\alpha_4 = \{0.5, 0.7, 0.9\}$ .

parameters	default	method	HGS	TRAF2
$B \in B_1, \alpha = \alpha_1$	$B = 100$	Forest	3.9%	3.6%
$B \in B_2, \alpha = \alpha_1$	$B = 100$	Forest	1.4%	1.6%
$B \in B_1, \alpha = \alpha_1$	$B = 100$	soft-VQ	1.3%	1.2%
$B \in B_2, \alpha = \alpha_1$	$B = 100$	soft-VQ	0.5%	0.2%
$\alpha \in \alpha_1, B = B_1$	$\alpha = 0.5$	Forest	2.9%	3.6%
$\alpha \in \alpha_2, B = B_1$	$\alpha = 0.5$	Forest	2.2%	2.1%
$\alpha \in \alpha_3, B = B_1$	$\alpha = 0.5$	Forest	1.7%	3.6%
$\alpha \in \alpha_4, B = B_1$	$\alpha = 0.5$	Forest	2.7%	2.9%
$\alpha \in \alpha_1, B = B_1$	$\alpha = 0.5$	soft-VQ	7.3%	8.6%
$\alpha \in \alpha_2, B = B_1$	$\alpha = 0.5$	soft-VQ	3.7%	1.3%
$\alpha \in \alpha_3, B = B_1$	$\alpha = 0.5$	soft-VQ	7.5%	10.8%
$\alpha \in \alpha_4, B = B_1$	$\alpha = 0.5$	soft-VQ	1.7%	0.6%

#### 6.4 Discussion

The results in Tables 1 and 2 reveal that the forest-based method is less robust. Actually, in Table 1 the forest gives similar to the soft-VQ, while in Table 2 the VQ-based method largely outperforms the forest in a range from 14% to 20%. The explanation of this phenomenon is the fact that we set the number of trees in the forest to  $B = 100$  the data proportion to train a tree at  $\alpha = 0.5$ . These values are well set in Table 1, but this is not true in Table 2. In order

to improve the chosen value, we could train the optimal value in a grid search, as it is done for the GMM in section 3.3.

We now discuss the fact that the standard deviation of the VQ-based methods is much higher than the forest and the random classification. The VQ methods are trained in an unsupervised context. The consequence being that cluster definition only depends on the random centroid initialization. Hence, the cell classification may strongly vary between two VQ realizations. On the other hand, both GMM and Forest are trained in a supervised manner. In such a case, clusters are not only driven by centroid initialization, but also by the class distributions. This constraint forces the clusters to converge to steeper results, where clusters are centered around the class mixtures or the class specificities. The consequence is a reduction of both the randomness of events and the standard deviation. Note that the random classification is based on a random class attribution to each cell. Hence, it is not surprising to have similar error rates between several consecutive experiments.

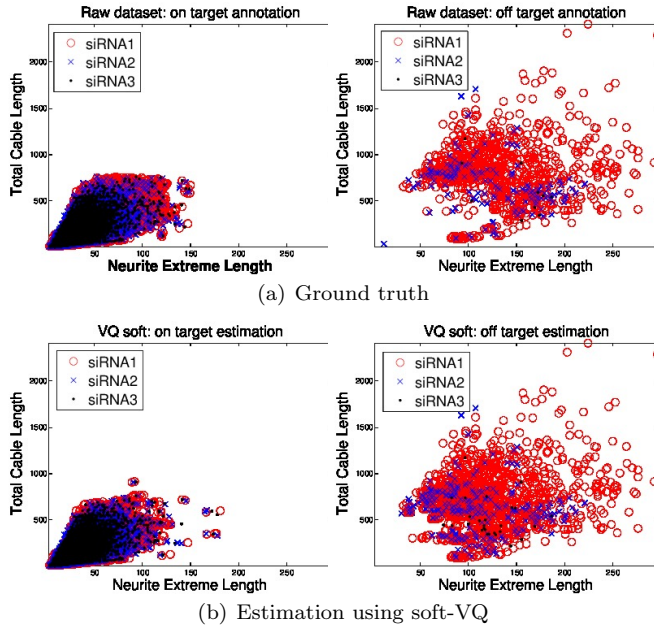


**Fig. 5** Classification results for the gene HGS: (a) The raw data set, (b) Estimation using soft Vector Quantization (soft-VQ).

Now, we address the convergence of Expectation-Maximization (EM). In Table 1, VQ+GMM outperforms VQ, but Forest outperforms Forest+GMM. On the contrary, in Table 2, VQ outperforms VQ+GMM while Forest+GMM outperforms Forest. The theory behind this results is that, using EM, the likelihood does not necessarily converge towards a global maximum. Instead,

any local extrema such as local maximum, local minimum or saddle point, may be reached. The consequence is that the likelihood may slightly decrease after an EM procedure, especially if the initialization is already interesting. In their works, McLachlan and Krishnan give such examples [21].

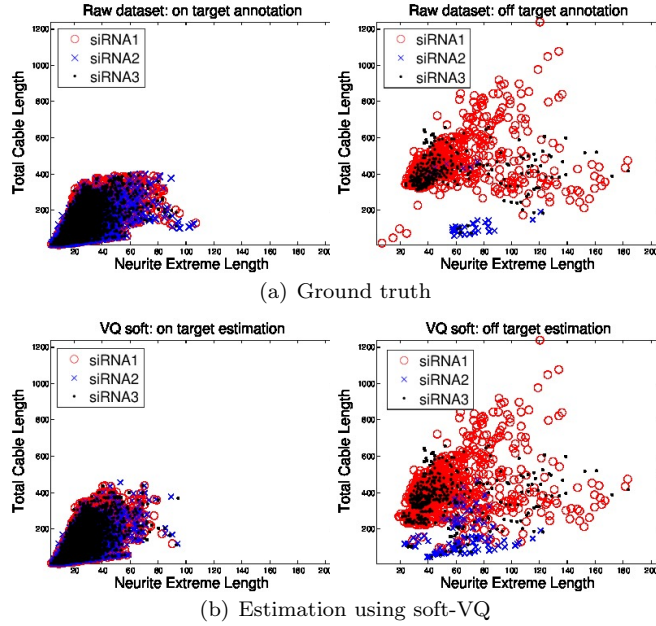


**Fig. 6** Classification results for the gene TRAF2: (a) The raw data set, (b) Estimation using soft Vector Quantization (soft-VQ).

## 7 Conclusion

We have proposed several implementations of a common idea to detect automatically the “off-target” population in a set of samples. One is based on Vector Quantization, and the other on a forest of decision trees. Both of these methods are able to cope with large data sets in high-dimension space.

A necessary condition common to all our methods is to have at least one phenotype which is the same for every RNA molecules. In other words, we force a cell to be considered as “off-target” from the moment a RNA molecule is not represented. However, these condition can be relaxed to extend the approach to more general situations. For instance, when a lots of different RNA molecules are used to knockdown a gene, we may be interested in considering a percentage of RNA molecules having similar phenotypic components instead of the majority. We could stipulate that, if 80% of the RNA molecules produce

the same phenotype, this phenotype is “on-target”. We want to point out that the rules (17) and (25) can easily be changed to use this soft criterion.

In the experimental sections, we compared our proposed models to a baseline based on a Gaussian Mixture Model (GMM) [6]. In addition, we proposed to initialize the GMM training step in a proper way, i.e. by using our proposed methods. These experiments have been conducted from a real data set which is made of cells in time-laps movies, as well as a semi-synthetic data set and a toy synthetic data set.

Our main conclusion is that the VQ-based method drastically outperforms the baseline [6]. The forest also provides good recognition performance, but the evaluation of the parameters are not so easy such that we had bad results on the real data set. An other argument that goes in favor of the VQ-based model, is that this model is very straightforward and simple to understand for non computer-scientists such as biologists. The forest approach may still exhibit interesting properties in different contexts, for instance if the feature space lacks a metric structure.

## References

1. D. Arthur, S. Vassilvitskii, “k-means++: the advantages of careful seeding”, Proceedings of the ACM-SIAM symposium on Discrete algorithms, p. 1027-1035, 2007.
2. C. Bakal, “Quantitative Morphological Signatures Define Local Signaling Networks Regulating Cell Morphology”, *Science*, vol. 316, p. 1753-1756, 2007
3. C.M. Bishop and I. Ulusoy, “Generative Versus Discriminative Methods for Object Recognition”, Conference on Computer Vision and Pattern Recognition, vol. 2, p. 258-265, 2005
4. L. Breiman, “Random forest”, *Machine Learning*, vol. 45, p. 5-32, 2001
5. L. Breiman, J.H. Friedman, R.A. Olshen, C.J. Stone, “Classification and regression trees”, Monterey, CA: Wadsworth & Brooks/Cole Advanced Books & Software, 1984
6. C. Collinet, *et al.*, “Systems survey of endocytosis by multiparametric image analysis”, *Nature*, vol. 464, p. 243-249, 2010.
7. A.P. Dempster, N.M. Laird, and D.B. Rubin, “Maximum Likelihood from Incomplete Data via the EM Algorithm”, *Journal of the Royal Statistical Society. Series B (Methodological)*, vol. 39(1), p. 1-38, 1977
8. C.J. Echeverri, *et al.*, “Minimizing the risk of reporting false positives in large-scale RNAi screens”, *Nature Methods*, vol. 3(10), p. 777-779, 2006.
9. Y. Freund, R.E. Schapire, “A Decision-Theoretic Generalization of On-Line Learning and an Application to Boosting”, *Journal of Computer and System Sciences*, vol. 55(1), p. 119-139, 1997
10. J.A. Hartigan, “Clustering algorithms”, John Wiley & Sons, Inc., 1975.
11. M. Held, *et al.*, “CellCognition: time-resolved phenotype annotation in high-throughput live cell imaging”, *Nature Methods*, 7, 747-754, 2010
12. A.L. Jackson and P.S. Linsley, “Recognizing and avoiding siRNA off-target effects for target identification and therapeutic application”, *Nature Reviews Drug Discovery*, vol. 9, p. 57-67, 2010
13. S. Kullback, “Letter to the Editor: The Kullback-Leibler distance”, *The American Statistician*, vol. 41(4), p. 340-341, 1987
14. I. Laptev, M. Marszalek, C. Schmid, and B. Rozenfeld, “Learning realistic human actions from movies”, International Conference on Computer Vision and Pattern Recognition, 2008.
15. R. Lefort, R. Fablet, J-M. Boucher, “Weakly supervised classification of objects in images using soft Random Forests”, European Conference on Computer Vision, 2010.

16. R. Lefort, R. Fablet, and J.M. Boucher, "Object recognition using proportion-based prior information: application to fisheries acoustics", *Pattern Recognition Letters*, vol. 32(2), p. 153-158, 2011.
17. R. Lefort, F. Fleuret, "treeKL: A distance between high dimension empirical distributions", *Pattern Recognition Letters*, 34(2), p. 140-145, 2013.
18. D. Lowe, "Object recognition with informative features and linear classification", *International Conference on Computer Vision and Pattern Recognition*, 1999.
19. E. Lughofer, "Extensions of Vector Quantization for Incremental Clustering", *Pattern Recognition*, vol. 41(3), p. 995-1011, 2008.
20. E. Lughofer, "eVQ-AM: An Extended Dynamic Version of Evolving Vector Quantization", *IEEE Conference on Evolving and Adaptive Intelligent Systems*, p. 40-47, 2013.
21. G. J. McLachlan, T. Krishnan, "The EM Algorithm and Extensions", New York, NY: John Wiley & Sons, 2nd Edition, 2008.
22. P.C. Mahalanobis, "On the generalised distance in statistics", *Proceedings of the National Institute of Sciences of India*, vol. 2(1), p. 49-55, 1936
23. F. Moosman, E. Nowak, F. Jurie, "Randomized clustering forests for image classification", *IEEE Transactions on Pattern Analysis and Machine Intelligence*, 30(9), 2008
24. B. Neumann, *et al.*, "Phenotypic profiling of the human genome by time-lapse microscopy reveals cell division genes", *Nature*, 464, p. 721-72, 2010
25. A. Orvedahl, *et al.*, "Image-based genome-wide siRNA screen identifies selective autophagy factors", *Nature*, vol. 480, p. 113-117, 2011.
26. E. Parzen, "On estimation of a probability density function and mode", *Annals of Mathematical Statistics*, vol. 33, p. 1065-1076, 1962
27. O. Pertz, *et al.*, "Spatial mapping of the neurite and soma proteomes reveals a functional Cdc42/Rac regulatory network", *The National Academy of Sciences of the USA*, 105, 1931-1936, 2008
28. J. Salma, *et al.*, "Computational analysis and predictive modeling of small molecule modulators of microRNA", *Journal of Cheminformatics*, vol. 4(16), 2012.
29. B. Schölkopf, A.J. Smola, "Learning With Kernels: Support Vector Machines, Regularization, Optimization and Beyond", MIT Press, 2002.
30. J. Yan, *et al.*, "Transcription factor binding in human cells occurs in dense clusters formed around cohesin anchor sites", *Cell*, vol. 154(4), p. 801-813, 2013.
31. Z. Yin, *et al.*, "A screen for morphological complexity identifies regulators of switch-like transitions between discrete cell shape", *Nature Cell Biology*, vol. 15(7), p. 860-871, 2013.
32. C. Yizong, "Mean Shift, Mode Seeking, and Clustering", *IEEE Transactions on Pattern Analysis and Machine Intelligence*, vol. 17(8), p. 790-799, 1995.